Few-Body Syst (2015) 56:447–453
DOI 10.1007/s00601-015-0976-x

**M. Engelhardt · B. Musch · P. Hägler · J. Negele · A. Schäfer**

# Lattice QCD Studies of Transverse Momentum-Dependent Parton Distribution Functions

Received: 1 October 2014 / Accepted: 3 April 2015 / Published online: 24 April 2015


**Abstract** Transverse momentum-dependent parton distributions (TMDs) relevant for semi-inclusive deep inelastic scattering and the Drell–Yan process can be defined in terms of matrix elements of a quark bilocal operator containing a staple-shaped gauge link. Such a definition opens the possibility of evaluating TMDs within lattice QCD. By parametrizing the aforementioned matrix elements in terms of invariant amplitudes, the problem can be cast in a Lorentz frame suited for the lattice calculation. Results for selected TMD observables are presented, including a particular focus on their dependence on a Collins–Soper-type evolution parameter, which quantifies proximity of the staple-shaped gauge links to the light cone.

## 1 Introduction

In the description of hadron structure, transverse momentum-dependent parton distribution functions [1] (TMDs) play a role complementary to generalized parton distributions (GPDs). Whereas GPDs encode information about the transverse spatial distribution of partons, TMDs contain information about the transverse momentum distribution of partons. As detailed further below, the definition of TMDs involves a number of subtleties not encountered in the case of GPDs, which also must be taken into account in formulating corresponding lattice QCD calculational schemes. Cast in a Lorentz frame in which the hadron of mass $m_h$ propagates with a large momentum in 3-direction, $P^+ \equiv (P^0 + P^3)/\sqrt{2} \gg m_h$, the quark momentum components scale such that TMDs are principally functions $f(x, k_T)$ of the quark longitudinal momentum fraction $x = k^+/P^+$ and the quark transverse momentum vector $k_T$, with the dependence on the component $k^- \equiv (k^0 - k^3)/\sqrt{2} \ll m_h$ becoming ignorable in this limit. $f(x, k_T)$ will thus be regarded as having been integrated over $k^-$.

Experimentally, TMDs manifest themselves in angular asymmetries observed in processes such as semi-inclusive deep inelastic scattering (SIDIS) and the Drell–Yan (DY) process. Corresponding signatures have emerged at COMPASS, HERMES and JLab [2–4], and that has motivated targeting a significant part of the physics program at future experiments in this direction, e.g., at the upgraded JLab 12 GeV facility and at the proposed electron-ion collider (EIC). To relate the experimental signature to the hadron structure encoded in TMDs, a suitable factorization framework is required. One possible such framework which is particularly well-suited for connecting phenomenology to a lattice QCD calculation has been advanced in [5–8]. Factorization

M. Engelhardt (✉)
Department of Physics, New Mexico State University, Las Cruces, NM 88003, USA
E-mail: engel@nmsu.edu

B. Musch · P. Hägler · A. Schäfer
Institut für Theoretische Physik, Universität Regensburg, 93040 Regensburg, Germany

J. Negele
Center for Theoretical Physics, Massachusetts Institute of Technology, Cambridge, MA 02139, USA

in the TMD context is considerably more involved than standard collinear factorization, with the resulting TMDs in general being process-dependent, via initial and/or final state interactions between the struck quark and the hadron remnant.

The main thrust of the present work lies in casting the phenomenological definition of TMDs into a form amenable to evaluation within lattice QCD, and presenting exploratory results for selected TMD observables. Time-reversal odd (T-odd) observables such as the Sivers and Boer-Mulders shifts are discussed. A detailed account of some aspects of this work was presented in [9].

## 2 Definition of TMD Observables

The fundamental correlator defining TMDs is of the form

$$\Phi^{[\Gamma]}(x, k_T, P, S, \ldots) = \int \frac{d^2 b_T}{(2\pi)^2} \int \frac{d(b\cdot P)}{(2\pi) P^+} \exp\left(ix(b\cdot P) - ib_T \cdot k_T\right) \left. \frac{\widetilde{\Phi}^{[\Gamma]}_{\text{unsubtr.}}(b, P, S, \ldots)}{\widetilde{\mathcal{S}}(b^2, \ldots)} \right|_{b^+=0} \tag{1}$$

with

$$\widetilde{\Phi}^{[\Gamma]}_{\text{unsubtr.}}(b, P, S, \ldots) \equiv \frac{1}{2} \langle P, S | \, \bar{q}(0) \, \Gamma \, \mathcal{U}[0, \ldots, b] \, q(b) \, | P, S \rangle \tag{2}$$

where $S$ denotes the hadron spin and $\Gamma$ an arbitrary $\gamma$-matrix structure. Heuristically, the Fourier-transformed bilocal quark bilinear operator counts quarks of momentum $k$, with $\Gamma$ controlling the spinor components involved. However, gauge invariance additionally enforces the introduction of the gauge connection $\mathcal{U}$, the precise path of which is not specified at this point; its choice will be guided by the physical process under consideration. In turn, the presence of $\mathcal{U}$ introduces divergences additional to the wave function renormalizations of the quark operators (this is indicated by the subscript "unsubtr."); these divergences accordingly are compensated by the additional "soft factor" $\widetilde{\mathcal{S}}$. Here, $\widetilde{\mathcal{S}}$ does not need to be specified in detail, since only appropriate ratios in which the soft factors cancel will ultimately be considered. Finally, $\Phi^{[\Gamma]}(x, k_T, P, S, \ldots)$ is, as noted further above, a function only of the three quark momentum components contained in $x$ and $k_T$, whereas the small component $k^-$ is integrated over; thus, in its Fourier transform, the conjugate component $b^+$ is set to zero, as written in (1).

Decomposing the correlator $\Phi^{[\Gamma]}(x, k_T, P, S, \ldots)$ into the relevant Lorentz structures yields the TMDs as coefficient functions. Quoting only the structures relevant for the following discussion,

$$\Phi^{[\gamma^+]} = f_1 - \left[ \frac{\epsilon_{ij} k_i S_j}{m_h} f_{1T}^{\perp} \right]_{\text{odd}} \tag{3}$$

$$\Phi^{[i\sigma^{i+}\gamma^5]} = S_i h_1 + \frac{(2k_i k_j - k_T^2 \delta_{ij}) S_j}{2m_h^2} h_{1T}^{\perp} + \frac{\Lambda k_i}{m_h} h_{1L}^{\perp} + \left[ \frac{\epsilon_{ij} k_j}{m_h} h_1^{\perp} \right]_{\text{odd}} \tag{4}$$

where $\Lambda$ denotes the hadron helicity (i.e., $S^+ = \Lambda P^+/m_h$, $S^- = -\Lambda m_h/2P^+$). In particular, the two TMDs $f_{1T}^{\perp}$ and $h_1^{\perp}$ are odd under time reversal, and can only arise if a mechanism is operative which breaks time-reversal invariance. The former TMD, characterizing the unpolarized distribution of quarks in a transversely polarized hadron, is the Sivers function, whereas the latter TMD, characterizing the distribution of transversely polarized quarks in an unpolarized hadron, is the Boer-Mulders function.

Up to this point, no reference has been made to a physical process which may be parametrized by the TMDs. Such a connection requires a factorization framework which allows one to separate the description of the physical process into the hard, perturbative vertex, a TMD encoding the structure of the hadron, and further components such as fragmentation functions describing the hadronization of the struck quark. For selected processes, including semi-inclusive deep inelastic scattering (SIDIS) and the Drell–Yan (DY) process, factorization arguments have been constructed, one possible approach having been advanced, e.g., in [5–8]. A crucial aspect in the description of, e.g., SIDIS is the inclusion of final-state gluon exchanges between the struck quark and the hadron remnant. These final state effects break time-reversal invariance and thus lead to nontrivial T-odd TMDs. At a formal level, a resummation of these gluon exchanges in the spirit of an eikonal approximation yields a Wilson line approximately following the trajectory of the struck quark, close to the light cone. This motivates a specific choice for the gauge connection between the quark operators in (2). Namely, parallel Wilson lines are attached to both of the quark operators, extending to large distances along a direction $v$ close to the light cone; at the far end, these lines are connected by a Wilson line in the $b$ direction to

maintain gauge invariance. The result is a staple-shaped connection $\mathcal{U}[0, \eta v, \eta v + b, b]$, where the path links the positions in the argument of $\mathcal{U}$ with straight line segments, and $\eta$ parametrizes the length of the staple. Formally, thus, it is the introduction of the additional vector $v$ which breaks the symmetry under time reversal and makes nonvanishing Sivers and Boer-Mulders effects possible.

At first sight, the most convenient choice for the staple direction $v$ would seem to be a light-like vector. However, beyond tree level, this introduces rapidity divergences which require regularization. One advantageous way to accomplish this is to take $v$ slightly off the light cone into the space-like region [5,6], with perturbative evolution equations governing the approach to the light cone [7]. Within this scheme, common TMDs describe both SIDIS and DY, except that in the DY process, it is initial state interactions which play a crucial role; correspondingly, the staple direction $v$ is inverted and the T-odd TMDs acquire a minus sign. A scheme in which $v$ (along with the quark operator separation $b$) is generically space-like is also attractive from the point of view of lattice QCD, as discussed further below. It will thus constitute the starting point for the development of the lattice calculation. A useful parameter characterizing how close $v$ is to the light cone is the Collins–Soper evolution parameter

$$\hat{\zeta} = v \cdot P/(|v|\,|P|), \tag{5}$$

in terms of which the light cone is approached for $\hat{\zeta} \to \infty$.

The correlator (2) can be decomposed in terms of invariant amplitudes $\widetilde{A}_{iB}$. Listing only the components relevant for the Sivers and Boer-Mulders effects,

$$\frac{1}{2P^+}\widetilde{\Phi}^{[\gamma^+]}_{\text{unsubtr.}} = \widetilde{A}_{2B} + im_h\epsilon_{ij}b_i S_j \widetilde{A}_{12B} \tag{6}$$

$$\frac{1}{2P^+}\widetilde{\Phi}^{[i\sigma^{i+}\gamma^5]}_{\text{unsubtr.}} = im_h\epsilon_{ij}b_j\widetilde{A}_{4B} - S_i\widetilde{A}_{9B} - im_h\Lambda b_i\widetilde{A}_{10B} + m_h[(b\cdot P)\Lambda - m_h(b_T\cdot S_T)]b_i\widetilde{A}_{11B}. \tag{7}$$

These amplitudes are useful in that they can be evaluated in any desired Lorentz frame, including a frame which is particularly suited for the lattice calculation. On the other hand, in view of (3)–(4), they are clearly closely related to Fourier-transformed TMDs. Performing the corresponding algebra, and quoting only the components necessary for defining the Sivers and Boer-Mulders shifts below,

$$\tilde{f}_1^{[1](0)}\left(b_T^2, \hat{\zeta}, \ldots, \eta v\cdot P\right) = 2\widetilde{A}_{2B}\left(-b_T^2, b\cdot P = 0, \hat{\zeta}, \eta v\cdot P\right)/\widetilde{\mathcal{S}}\left(b^2, \ldots\right) \tag{8}$$

$$\tilde{f}_{1T}^{\perp[1](1)}\left(b_T^2, \hat{\zeta}, \ldots, \eta v\cdot P\right) = -2\widetilde{A}_{12B}\left(-b_T^2, b\cdot P = 0, \hat{\zeta}, \eta v\cdot P\right)/\widetilde{\mathcal{S}}(b^2, \ldots) \tag{9}$$

$$\tilde{h}_1^{\perp[1](1)}\left(b_T^2, \hat{\zeta}, \ldots, \eta v\cdot P\right) = 2\widetilde{A}_{4B}\left(-b_T^2, b\cdot P = 0, \hat{\zeta}, \eta v\cdot P\right)/\widetilde{\mathcal{S}}(b^2, \ldots) \tag{10}$$

where the generic Fourier-transformed TMD is defined as [10]

$$\tilde{f}^{[1](n)}\left(b_T^2, \ldots\right) = n!\left(-\frac{2}{m_h^2}\partial_{b_T^2}\right)^n \int_{-1}^{1} dx \int d^2k_T\, e^{ib_T\cdot k_T}\, f\left(x, k_T^2, \ldots\right). \tag{11}$$

The $b_T \to 0$ limit formally yields $k_T$-moments of TMDs. However, this limit contains additional singularities, which one can view as being regulated by a finite $b_T$. Here, results will only be given at finite $b_T$. Note the presence of the soft factors $\widetilde{\mathcal{S}}$ on the right-hand sides of (8)–(10). One can construct observables in which the soft factors cancel by normalizing the (Fourier-transformed) Sivers and Boer-Mulders functions (9) and (10) by the unpolarized TMD (8), which essentially counts the number of valence quarks[1]. Thus, one defines the "generalized Sivers shift"

$$\langle k_y\rangle_{TU}\left(b_T^2, \ldots\right) \equiv m_h\frac{\tilde{f}_{1T}^{\perp[1](1)}\left(b_T^2, \ldots\right)}{\tilde{f}_1^{[1](0)}\left(b_T^2, \ldots\right)} = -m_h\frac{\widetilde{A}_{12B}\left(-b_T^2, 0, \hat{\zeta}, \eta v\cdot P\right)}{\widetilde{A}_{2B}\left(-b_T^2, 0, \hat{\zeta}, \eta v\cdot P\right)} \tag{12}$$

[1] That the purely multiplicative nature of the soft factors in this continuum construction transfers verbatim to the lattice formulation of QCD is a working assumption, to be investigated in more detail in future work.

which is the regularized, finite-$b_T$ generalization of the "Sivers shift"

$$m_h \frac{\tilde{f}_{1T}^{\perp[1](1)}(0,\ldots)}{\tilde{f}_1^{[1](0)}(0,\ldots)} = \frac{\int dx \int d^2k_T\, k_y \Phi^{[\gamma^+]}(x, k_T, S_T = (1,0))}{\int dx \int d^2k_T\, \Phi^{[\gamma^+]}(x, k_T, S_T = (1,0))}, \tag{13}$$

which, in view of the right-hand side, formally represents the average transverse momentum of unpolarized ("$U$") quarks orthogonal to the transverse ("$T$") spin of the hadron, normalized to the corresponding number of valence quarks. In the interpretation of (13), it should be noted that the numerator sums over the contributions from quarks and antiquarks, whereas the denominator contains the difference between quark and antiquark contributions, thus giving the number of valence quarks. Analogously, one can also extract the generalized Boer-Mulders shift

$$\langle k_y \rangle_{UT}\left(b_T^2, \ldots\right) = m_h \frac{\widetilde{A}_{4B}\left(-b_T^2, 0, \hat{\zeta}, \eta v\cdot P\right)}{\widetilde{A}_{2B}\left(-b_T^2, 0, \hat{\zeta}, \eta v\cdot P\right)}. \tag{14}$$

Besides the soft factors, the ratios (12) and (14) also cancel multiplicative wave function renormalization constants attached to the quark operators in (2).

## 3 Lattice Evaluation and Results

The formal framework laid out above provides all the necessary elements for a lattice QCD evaluation of generalized shifts such as (12) and (14). One calculates hadron matrix elements of the type (2) and then decomposes them into invariant amplitudes, as given in (6)–(7). For this to be possible, it is crucial to work in a scheme where the four-vectors $b$ and $v$ are generically space-like, for the following reason: By employing a Euclidean time coordinate to project out hadron ground states via Euclidean time evolution, lattice QCD cannot straightforwardly accomodate operators containing Minkowski time separations. The operator of which one takes matrix elements thus has to be defined at a single time. Only if both $b$ and $v$ are space-like is there no obstacle to boosting the problem to a Lorentz frame in which $b$ and $v$ are purely spatial, and evaluating $\widetilde{\Phi}^{[\Gamma]}_{\text{unsubtr.}}$ in that frame. The results extracted for the invariant amplitudes $\widetilde{A}_{iB}$ are then immediately valid also in the original frame in which (2) was initially defined, thus completing the determination of quantities of the type (12) and (14).

Since, in a numerical lattice calculation, the staple extent $\eta$ necessarily remains finite, two extrapolations must be performed from the generated data, namely, the one to infinite staple length, $\eta \to \infty$, and the extrapolation of the staple direction towards the light cone, $\hat{\zeta} \to \infty$. As shown below, the former extrapolation is under control for a range of parameters used in this work, whereas the latter presents a challenge, owing to the limited set of hadron momenta $P$ accessible with sufficient statistical accuracy. The lattice data shown in the following were obtained on three MILC 2+1-flavor gauge ensembles [11] with a lattice spacing of $a = 0.12\,\text{fm}$, corresponding to pion masses $m_\pi = 369\,\text{MeV}$ and $m_\pi = 518\,\text{MeV}$, with two lattice sizes used in the former case, $20^3 \times 64$ and $28^3 \times 64$. For $m_\pi = 518\,\text{MeV}$, the lattice size is $20^3 \times 64$. The heavier pion mass ensemble, fraught with less statistical uncertainty, provides the largest $\hat{\zeta}$ values, namely, $\hat{\zeta} = 0.78$ for a nucleon and $\hat{\zeta} = 2.03$ for a pion.

Figures 1 and 2 show representative results for the generalized Sivers and Boer-Mulders shifts (12) and (14) in the nucleon. Results for the isovector, $u-d$ quark combination are displayed; in this channel, couplings of the operator insertion to disconnected quark loops in the nucleon, which have been discarded, cancel. Figure 1 (left) displays the dependence of the Sivers shift on the staple extent for a given quark separation $b_T$ and a given staple direction characterized by $\hat{\zeta}$. The T-odd behavior of this observable is evident, with $\eta \to \infty$ corresponding to the SIDIS limit, whereas $\eta \to -\infty$ yields the DY limit. The data level off to approach clearly identifiable plateaux as the staple length grows. The limiting SIDIS and DY values, represented by the open symbols, are extracted by imposing antisymmetry in $\eta$, allowing one to appropriately average the $\eta \to \pm\infty$ plateau values. Figure 1 (right) summarizes the results in the SIDIS limit for different $b_T$ at a given $\hat{\zeta}$, where the shaded area below $|b_T| \approx 0.25\,\text{fm}$ indicates the region where the results may be significantly affected by finite lattice cutoff effects.

Figure 2 summarizes the dependence of the Sivers and Boer-Mulders shifts on the Collins–Soper evolution parameter $\hat{\zeta}$, for all three ensembles considered, with $|b_T|$ kept fixed. Note that the relevant data in the left-hand panel, displaying the Sivers shift, are represented by the full symbols; the empty symbols correspond to

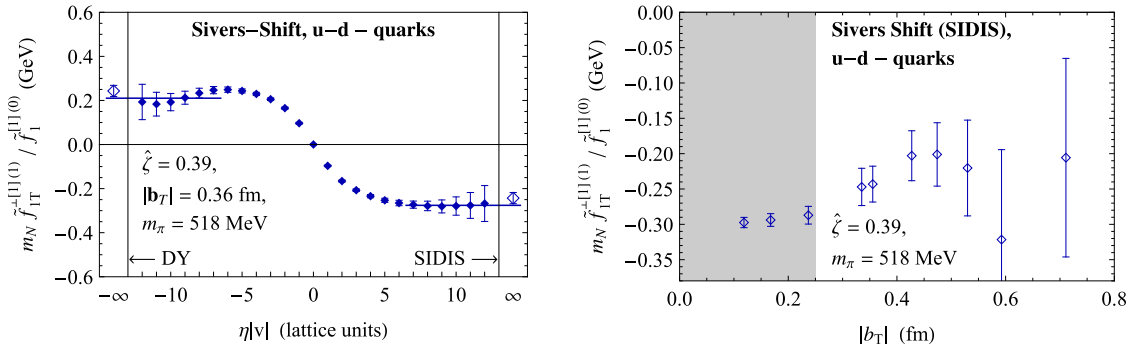


**Fig. 1** Dependence of the generalized Sivers shift on the staple extent (*left*) and on the quark separation $b_T$ in the $\eta \to \infty$ SIDIS limit (*right*); from [9]

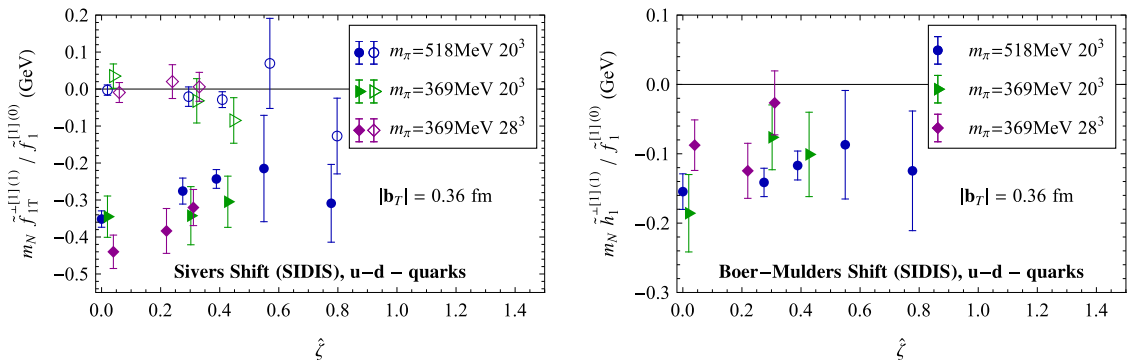


**Fig. 2** Results for Sivers and Boer-Mulders shifts as a function of $\hat{\zeta}$ for a fixed $b_T$ for all ensembles; from [9]

a certain partial contribution to the Sivers shift which vanishes at $\hat{\zeta} = 0$, but dominates the quantity at large $\hat{\zeta}$; comparison of the full Sivers shift with the partial contribution thus can give an indication of convergence towards the large $\hat{\zeta}$ limit. For further details, cf. [9]. The signal for the shifts quickly deteriorates as the nucleon momentum $P$, and thus $\hat{\zeta}$, is increased. No clear trend can be identified at the present level of accuracy as $\hat{\zeta}$ rises, and connecting with perturbative evolution equations at large $\hat{\zeta}$ will clearly represent a challenge for the present approach. Within the (sizeable) uncertainties, no significant variation can be discerned as one changes the pion mass or the spatial extent of the lattice. In the isovector channel displayed, the signal for the Sivers shift is of higher quality than the one for the Boer-Mulders shift. One reason for this is that, if one separates the $u$- and $d$-quark contributions, the Sivers shifts in the two cases are of opposite sign (thus reinforcing each other in the $u - d$ difference), whereas the Boer-Mulders shifts are of the same sign, thus canceling each other to some extent. Note that the lattice results obtained in this work are compatible with phenomenological analyses of experimental SIDIS data [12,13], in spite of the variety of systematic effects which would still need to be taken into account for a fully quantitative comparison.

To obtain further insight regarding the large $\hat{\zeta}$ limit, also a study of the Boer-Mulders shift in the pion on the $m_\pi = 518\,\text{MeV}$ ensemble was performed. The lower mass of the pion compared with the one of the nucleon (note that the hadron mass enters the denominator of $\hat{\zeta}$ in (5)), and the accumulation of higher statistics permitted the treatment of higher $\hat{\zeta}$ with improved accuracy. Figure 3 shows representative results, for $u$-quarks alone; in the pion case, the isovector combination vanishes. The corresponding disconnected contributions are not included. Remarkably, the $b_T$-dependence of the Boer-Mulders shift flattens as $\hat{\zeta}$ is increased, and the data for different $\hat{\zeta}$ approach each other at large $b_T$. It would be useful to understand this behavior in detail. Focusing on a particular value of $b_T$, Figure 3 (right) displays the $\hat{\zeta}$-dependence of both the full Boer-Mulders shift as well as the partial contribution already alluded to further above, along with corresponding extrapolations. In the pion case, the partial contribution already furnishes roughly one half of the full shift at the highest $\hat{\zeta}$ reached, signaling that the calculation has covered a significant part of the evolution to large $\hat{\zeta}$. Still, the pion momenta employed are too small to guarantee a reliable connection to perturbative evolution; the functional

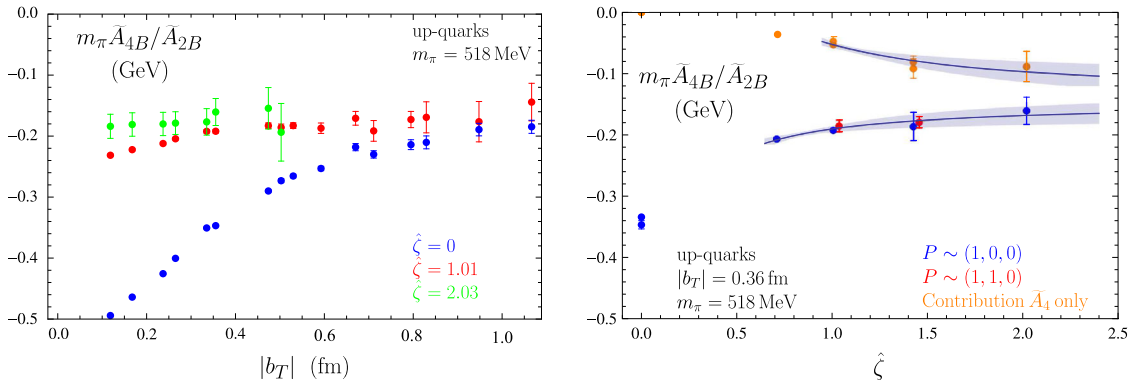


**Fig. 3** Boer-Mulders shift in the pion in the SIDIS limit, for $u$-quarks; *left*: dependence on the quark separation $b_T$ for several $\hat{\zeta}$, *right*: extrapolation of the $\hat{\zeta}$-dependence at a fixed $b_T$, for details, cf. main text

form $a + b/\hat{\zeta}$ employed in the fits thus should be regarded as no more than an ad hoc ansatz. The fits converge to compatible values, $-0.146(26)$ and $-0.141(36)$ for the full and the partial shifts, respectively; this accords with expectations and demonstrates that lattice calculations can achieve a signal for the Boer-Mulders shift of sufficient quality such that it survives taking the $\hat{\zeta} \to \infty$ limit.

## 4 Summary and Outlook

This exploratory study of TMDs within lattice QCD, employing staple-shaped gauge connections to incorporate final/initial state effects (for SIDIS/DY), has provided first results for T-odd Sivers and Boer-Mulders observables. To cancel soft factors and multiplicative renormalization constants, appropriate ratios of Fourier-transformed TMDs ("generalized shifts", cf. (12) and (14)) were constructed. The staple direction $v$ was taken to be generically space-like, with the light-cone limit to be approached by extrapolation in the Collins–Soper parameter $\hat{\zeta}$. This extrapolation has to be performed in addition to the one to infinite staple extents $\eta$. While the latter extrapolation is under control for a range of parameters considered in this work, the limit $\hat{\zeta} \to \infty$ clearly presents a challenge for the approach presented here. However, under favorable conditions, as demonstrated by a dedicated study of the Boer-Mulders shift in a pion, it is possible to reach tentative conclusions concerning the $\hat{\zeta} \to \infty$ limit. Current efforts are focused on exploring lighter pion masses, as well as testing the universality of the results when the lattice discretization (spacing, fermion action) is varied.

**Acknowledgments** Computations were performed employing resources provided by the U.S. DOE through USQCD at Jefferson Lab, using the Chroma software suite [14]. Support by the Heisenberg-Fellowship program of the DFG (P.H.), SFB/TRR-55 (A.S.), and the U.S. DOE and the Office of Nuclear Physics through Grants DE-FG02-96ER40965 (M.E.) and DE-SC0011090 (J.N.), as well as through contract DE-AC05-06OR23177, under which Jefferson Science Associates, LLC, operates Jefferson Laboratory (B.M.), is acknowledged.

## References

1. Boer, D., Diehl, M., Milner, R., Venugopalan, R., Vogelsang, W., et al.: Gluons and the quark sea at high energies: distributions, polarization, tomography. arXiv:1108.1713 (2011)
2. Alekseev, M. et al.COMPASS Collaboration: Collins and Sivers asymmetries for pions and kaons in muon-deuteron DIS. Phys. Lett. **B673**, 127–135 (2009)
3. Airapetian, A. et al. HERMES Collaboration: Observation of the naive-T-odd Sivers effect in deep-inelastic scattering. Phys. Rev. Lett. **103**, 152002 (2009)
4. Avakian, H. et al. CLAS Collaboration: Measurement of single and double spin asymmetries in deep inelastic pion electroproduction with a longitudinally polarized target. Phys. Rev. Lett. **105**, 262002 (2010)
5. Aybat, S.M., Rogers, T.C.: TMD parton distribution and fragmentation functions with QCD evolution. Phys. Rev. D **83**, 114042 (2011)
6. Collins, J.C.: *Foundations of Perturbative QCD*. Cambridge University Press, Cambridge (2011)
7. Aybat, S.M., Collins, J.C., Qiu, J.-W., Rogers, T.C.: The QCD evolution of the Sivers function. Phys. Rev. **D 85**, 034043 (2012)

8. Collins, J.C., Rogers, T.C.: Equality of two definitions for transverse momentum dependent parton distribution functions. Phys. Rev. **D 87**, 034018 (2013)
9. Musch, B., Hägler, P., Engelhardt, M., Negele, J.W., Schäfer, A.: Sivers and Boer-Mulders observables from lattice QCD. Phys. Rev. **D 85**, 094510 (2012)
10. Boer, D., Gamberg, L., Musch, B., Prokudin, A.: Bessel-weighted asymmetries in semi inclusive deep inelastic scattering. JHEP **1110**, 021 (2011)
11. Aubin, C., Bernard, C., DeTar, C., Osborn, J., Gottlieb, S., Gregory, E., Toussaint, D., Heller, U., Hetrick, J., Sugar, R.: Light hadrons with improved staggered quarks: approaching the continuum limit. Phys. Rev. **D 70**, 094505 (2004)
12. Anselmino, M., Boglione, M., D'Alesio, U., Melis, S., Murgia, F., Prokudin, A.: Sivers distribution functions and the latest SIDIS data. arXiv:1107.4446 (2011)
13. Barone, V., Melis, S., Prokudin, A.: The Boer-Mulders effect in unpolarized SIDIS: an analysis of the COMPASS and HERMES data on the cos 2 phi asymmetry. Phys. Rev. **D 81**, 114026 (2010)
14. Edwards, R.G., Joó, B. SciDAC Collaboration: The Chroma software system for lattice QCD. Nucl. Phys. Proc. Suppl. **140**, 832–834 (2005)